T. vaginalis: Monolayer and cluster formation - ultrastructural aspects using HR-SEM

Sharmila Ortiz , Raphael Verdan , Fabio da Silva de Azevedo Fortes , Marlene Benchimol *

Posted Date: 3 October 2023

doi: 10.20944/preprints202309.2050.v1

Keywords: anaerobic parasites; pathogenicity; cell communication; cadherins; high-resolution SEM; Trichomonas adhesion.

Article

T. vaginalis: Monolayer and Cluster Formation-Ultrastructural Aspects Using HR-SEM

Sharmila Fiama das Neves Ortiz[1], Raphael Verdan [1], Fabio da Silva de Azevedo Fortes [2,4] and Marlene Benchimol [2,3,*]

[1] Laboratório de Ultraestrutura Celular Hertha Meyer, Instituto de Biofísica Carlos Chagas Filho, Centro de Pesquisa em Medicina de Precisão, Universidade Federal do Rio de Janeiro, Rio de Janeiro 21941-901, Brazil
[2] BIOTRANS-CAXIAS, Universidade do Grande Rio. UNIGRANRIO, Rio de Janeiro 96200-000, Brazil
[3] Instituto Nacional de Ciência e Tecnologia em Biologia Estrutural e Bioimagens e Centro Nacional de Biologia Estrutural e Bioimagens, Universidade Federal do Rio de Janeiro, Rio de Janeiro, RJ, Brazil
[4] Laboratório de Terapia e Fisiologia Celular e Molecular, Departamento de Biologia, Faculdade de Ciências Biológicas e Saúde, Universidade do Estado do Rio de Janeiro, Rio de Janeiro 23070-200, Brazil
* Correspondence: Email: marlenebenchimol@gmail.com; FAX: +55 21 25544716

Abstract: *Trichomonas vaginalis* is an extracellular parasite protozoan that causes human trichomoniasis, a sexually transmitted infection (STI) that affects approximately 200 million people worldwide. The presence of *T. vaginalis* adhesion to inert substrates has been described in several reports. Still, very few studies on cluster formation and more detailed analyses of the contact regions between the membranes of the parasites in these aggregate formations have not been carried out. We analyzed the formation of parasite monolayers and clusters using high-resolution scanning electron microscopy, transmission electron microscopy, cytochemistry, TEM tomography, and dye injection. Here, we show the formation of a monolayer of tightly adherent cells, epithelium-like, when the parasites are in contact with an inert material. Based on this observation, we analyzed whether this monolayer behaves as an epithelium, analyzing cell junctions, cell communication, and ultrastructural aspects. We also analyzed the cluster formation and the morphological characteristics of parasite aggregation observed in the culture supernatant. We report that monolayer formation differs from cluster formation in many aspects. The monolayers form strong adhesion, whereas the clusters have fragile attachments. There is no fusion or passage of molecules between neighbor-attached cells; there is no need for different strains to form filopodia, cytonemes, and extracellular vesicles during cluster formation.

Keywords: anaerobic parasites; pathogenicity; cell communication; cadherins; high-resolution SEM; *Trichomonas* adhesion

1. Introduction

Trichomonas vaginalis is a microaerophilic and extracellular parasite that colonizes the urogenital tract of humans (Figs. 1-3). Trichomoniasis affects more than 200 million people worldwide and is the third-most common sexually transmitted infection. As a result, women present frequent miscarriages, vaginal odor, and discharge, which can lead to infertility [1]. In addition, men, although usually asymptomatic, can present urethritis and prostate cancer [2]. *T. vaginalis* has also been described in the respiratory tract of adults and children [3,4].

Furthermore, trichomoniasis has been related to a greater predisposition to HIV (human immunodeficiency virus) and HPV (human papillomavirus)[5].

When *T. vaginalis* are grown in an axenic medium (TYM)[6], the cells are pyriform and free-swimming. However, the parasite changes its morphology under specific situations, such as intense stress due to starvation or drug treatment. In addition, virulent parasites change to an ameboid shape when in contact with target cells [7]. In addition, after the parasites adhere to host- cells, the trophozoites clump and transform into an ameboid shape [8]. Examination of human biopsies revealed that *T. vaginalis* trophozoites clustered in small areas of the mucosa.

 doi:10.20944/preprints202309.2050.v1

Several previous works debated the cytopathic effect of the parasite on the host cells. It has been suggested that damage to epithelial cells by *T. vaginalis* occurs initially through adhesion and clumping of parasites [8-10]. Consequently, host cells die, and cell debris are phagocyted [7].

T. vaginalis possesses surface proteins capable of binding to host cell glycosaminoglycans, and it has been discussed whether this interaction is a factor that increases the adherence of this parasite [11].

Here, we have focused on the formation of *T. vaginalis* clusters, which, although observed by several authors, were not analyzed in ultrastructural details. In addition, we searched whether communication between neighbor parasites could occur during this cell's contact.

2. Materials and Methods

The JT strain of *T. vaginalis* was isolated at the Hospital Universitário, Universidade Federal do Rio de Janeiro (Rio de Janeiro, Brazil), and it is a low virulent strain. The FMV1 strain is a fresh isolate kindly provided by Dr. J. Baptista (Instituto Oswaldo Cruz, Rio de Janeiro, Brazil). Dr. John F. Alderete kindly provided the fresh isolate T068. Based on the ability to destroy cells in culture, JT was previously classified as a low cytotoxic strain, whereas FMV1 and T068 were defined as cytotoxic strains [7]. Cells were cultivated in 15 mL Falcon® tubes containing TYM medium [6] at pH 6.2. The medium was supplemented with 10% FBS (Gibco, South America). Cells were maintained in 37°C incubators for 24-36 hours until they reached 80-100% confluency. Sterilized 13 mm round coverslips were placed inside a 24-well plate. The cells were detached from the tube wall by placing the tube on ice for 10 minutes and then centrifuging it at 1,000 g for 5 minutes. The cells were washed twice with phosphate-buffered saline (PBS) at pH 7.2 and 37°C and centrifuged. The pellet was resuspended in 400 µl of the supplemented medium. Subsequently, 100 µl of the cell suspension was pipetted onto each coverslip, and the well opening was sealed with Parafilm to reduce oxygen exposure. The coverslips were incubated in a 37°C incubator for 2-3 hours and fixed as necessary.

2.2. Fraction of T. vaginalis cytoskeleton

The trophozoites were detached from the tube wall as described above and were washed twice in PBS pH 7.2 with centrifugations at 1000 x g for 5 minutes at room temperature (RT). For the cytoskeleton extraction, the washed cells were then resuspended in 1 ml ice-cold PHEM buffer (60mM PIPES, 25mM HEPES, 10mM EGTA, and 4mM MgSO4·7H20) containing 30% glycerol (Sigma Aldrich, EUA), 2% Triton X-100 (Sigma Aldrich, USA), 2% Igepal (Sigma Aldrich, USA) including one 1x complete mini protease inhibitor (Sigma Aldrich, USA). The solution was vigorously vortexing at maximum speed for 2 minutes, incubated on ice for 2 minutes, and repeated two times. Then, the cytoskeleton-enriched fraction of *T. vaginalis* was washed in PBS pH 7,2 with centrifugation at 17000 x g 5 minutes, 4°C. The success of the extraction was confirmed through light microscopy.

2.3. Immunofluorescence microscopy

The coverslips with the cells were fixed with 4% paraformaldehyde in PHEM buffer (60 mM Pipes, 25 mM Hepes, 10 mM EGTA, and 2 mM $MgCl_2$) at pH 6.8 for 20 minutes. Then, they were washed thrice with PBS at pH 8.0 for 5 minutes each time. The cells were permeabilized with PBS 1% Triton X-100 (ThermoFisher, USA) and washed with PBS. Afterward, the cells were quenched with PBS containing 3% BSA and 0.01% Tween-20 (Sigma-Aldrich, USA) for 1 hour and washed as described above.

Next, the cells were incubated with an anti-pan cadherin monoclonal antibody (Abcam, UK) or anti-E-cadherin monoclonal antibody (Invitrogen, USA) at a dilution of 1:500, or E-cadherin Polyclonal Antibody (Invitrogen, USA, catalog number PA5-32178) at a dilution of 1:100 for 2 h overnight and then washed. The cells were then incubated with Alexa Fluor 546-conjugated anti-mouse or rabbit IgG antibody (Life Technologies) or Alexa Fluor 488 conjugated anti-mouse or anti-rabbit IgG antibody (Life Technologies) at a dilution of 1:400 in PBS containing 3% BSA for 1 hour. In addition, the following antibodies were also used: monoclonal anti-alpha-tubulin (TAT-1, kindly

 doi:10.20944/preprints202309.2050.v1

donated by Dr. Keith Gull) at a dilution of 1:400, Anti ZO-1 polyclonal (Invitrogen, catalog number 61-7300) was used diluted 1:100; Anti Claudina-3 polyclonal (Invitrogen, catalog number 34-1700), diluted 1:20. For nucleus visualization, 10 µg/ml of 4,6-diamidino-2-phenylindole (DAPI, Sigma-Aldrich, USA) was used. After the final washes in PBS, the slides were mounted with Prolong Gold Antifade (Invitrogen, USA). The cells were examined with a ZEISS ELYRA PS.1 microscope. In addition, immunofluorescence assays were performed, one with cells without permeabilization and another with live cells, maintaining the cells at low temperatures and incubating each antibody for 30 minutes.

2.4. High-resolution scanning electron microscopy (HR-SEM)

Cells were fixed in 2.5% glutaraldehyde in 0.1 M cacodylate buffer at pH 7.2. They were then post-fixed for 15 minutes in 1% OsO4, dehydrated in ethanol, and critically point-dried with liquid CO_2 (Leica EM CPD300, Leica, Germany). Subsequently, the cells were coated with an 8 nm thick layer of platinum and observed using a ZEISS AURIGA 40 high-resolution scanning electron microscope.

2.5. Transmission electron microscopy (TEM)

The cells were detached from the tube, washed with PBS at pH 7.2 at 37°C, and centrifuged. The pellet was resuspended in 2 ml of supplemented medium, and 1 ml was pipetted into each well of a 6-well plate or small Petri dish (9.6 cm^2). The well opening was sealed with Parafilm to reduce oxygen exposure, and the cells were left overnight. The cells were washed twice with PBS at pH 7.2 and 37°C and then fixed overnight at RT in 2.5% glutaraldehyde in 0.1 M cacodylate buffer. Next, a scraper was used carefully to detach the cells from the bottom of the plate. The supernatant was collected and transferred to a 15 mL Falcon® tube. Afterward, the cells were washed with 0.1 M cacodylate buffer and post-fixed for 15 minutes in 1% OsO_4 in 0.1 M cacodylate buffer containing 5 mM $CaCl_2$ and 0.8% potassium ferricyanide. The cells were then dehydrated in acetone and embedded in Epon. Ultrathin sections were harvested on 300 mesh copper grids, stained with 5% uranyl acetate and 1% lead citrate, and observed using a HITACHI HT 7800, Japan, transmission electron microscope.

2.6. Cluster formation

The tube containing the culture was placed in ice for 15 minutes to allow cell detachment from the tube's walls, followed by centrifugation at 2100 rpm for 5 minutes. The resulting pellet was resuspended in 1 ml of TYM medium supplemented with fetal bovine serum (FBS), and cell counting was performed, yielding a result of 9.10^6 cells/ml. Subsequently, 300 µl were inoculated into each 35 mm Petri dish (utilizing three dishes). The volume was adjusted to 4 ml and sealed with parafilm to achieve a reduced oxygen environment. The behavior of the cells was observed under an inverted light microscope. Within 5 minutes, all three Petri dishes already contained adhered cells on the plastic surface, exhibiting an ameboid shape with a 10-15% confluence. Plate 1 contained small clusters composed of 4-5 cells each.

Similarly, plate 2 presented small clusters, with a maximum of 10-12 protozoa per cluster. Plate 3 displayed a profile akin to that of plate 1. Subsequently, the plates were placed in an incubator at 37° C for 10 minutes. After this period, the supernatant of all plates contained 80-90% clusters, while the confluence of adhered cells reached approximately 50%. Plate 1 exhibited numerous large clusters, each comprising 100 or more cells. Plate 2 displayed many medium-sized clusters (40-50 protozoa), with fewer large clusters than plate 1. Plate 3 exhibited a profile like that of plate 2. The plates were then subjected to another 15 minutes of incubation at 37° C. The observed pattern closely resembled the previous analysis, with the notable distinction that the clusters present in all three plates were predominantly large, each containing more than 100 cells. Subsequently, the supernatant from the plates was carefully collected and transferred to 15 ml tubes, followed by centrifugation at 800 rpm for 5 minutes. The resulting pellet was fixed with 2.5% glutaraldehyde in 0.1 M sodium cacodylate buffer for 2 hours at RT, without prior washing steps, to prevent cluster disassociation.

 doi:10.20944/preprints202309.2050.v1

2.7. Ruthenium Red

Cells were fixed at RT in 2.5% glutaraldehyde in 0.1 M cacodylate buffer containing 1% ruthenium red (British Drug Houses, Ltd). The cells were washed with buffer and 1% OsO_4 containing 1% ruthenium red, dehydrated in acetone, and embedded in Epon. Ultrathin sections were harvested on 300 mesh copper grids and observed without staining.

2.8. Thiéry technique [12]

The parasites were fixed and processed as described above for TEM. Subsequently, 90 nm sections were collected on gold grids incubated for 20 minutes in a solution containing 1% periodic acid, washed, and incubated with 1% thiosemicarbazide in 10% acetic acid for 24 h. Successive washes were carried out in 10%, 5%, and 2% acetic acid for 10 min each. Afterward, they were incubated with 1% silver proteinate for 30 minutes protected from light. Subsequently, successive washes in distilled water were performed for 10 min each, and the unstained sections were observed on a Hitachi HT 7800 transmission electron microscope.

2.9. Immunolabeling

Cells were fixed overnight at RT in 0.5% glutaraldehyde plus 2% formaldehyde in 0.1 M cacodylate buffer, washed, dehydrated in acetone, and embedded in LR white resin. Ultrathin sections were harvested on 300 mesh, and labeling proceeded using the antibodies cited in the immunofluorescence section above.

2.10. Electron microscopy tomography

Cells were processed for TEM as described above, and blocks were used to obtain 200 nm thick sections, which were collected onto formvar-coated copper grids and stained with uranyl acetate and lead citrate. For alignment of the tilted views, colloidal gold particles (10 nm) were deposited on both sections' surfaces to be used as fiducial markers. A single-axis tilt series (+ -)55° with 2° increments) was produced from samples using Xplore D software and a Tecnai Spirit TEM (Thermofisher, USA) electron microscope operating at 120 kV. The IMOD software package performed all 3D reconstructions and subsequent 3D data analyses. ETOMO was used to generate a tomogram by R-weighted back projection. Virtual slices were manually segmented with 3DMOD to produce 3D models.

2.11. Dye Transfer (or Dye Injection)

Confluent cultures of *Trichomonas vaginalis* plated on 35 mm Petri dishes were injected with Lucifer Yellow CH (5% in 150 mM LiCl) (457.2 Da) using glass microelectrodes (resistance between 40-70 MΩ) by the application of short hyperpolarizing current pulses (0.1 nA, 100 milliseconds using a WPI amplifier, model 7060; USA). Fluorescence was observed on an Axiovert 100 microscope (Carl Zeiss, Oberkochen, Germany) equipped with appropriate filters (Zeiss BP450-490 / FT510 / LP520), and micrographs were taken using Image Pro Plus Program (Media Cybernetics, USA) 2 minutes after dye injection [13]. In measuring the degree of coupling, a minimum of 120 cells was injected in at least four independent experiments

3. Results

3.1. The monolayer formation

In the present study, we intended to follow the formation of the trichomonads monolayers and clumps using light and electron microscopy, among other techniques. Concerning the monolayer formation, we observed that the parasites are well spread out on the inert surface of the bottom of the flasks used. First, parasites project cell surface expansions and firmly adhere to the inert substrate. A transition from a pear-shaped to an amoeboid form is observed, and the cells spread with such

Preprints (www.preprints.org) | NOT PEER-REVIEWED | Posted: 3 October 2023 doi:10.20944/preprints202309.2050.v1

intensity that they become flattened. The cell contacts were followed by high-resolution scanning and transmission electron microscopy, and plasma membrane contact and interdigitations were formed. Initially, the single cells exhibited a routine morphology, presenting four anterior flagella and one recurrent flagellum, and are pear-shaped (Fig. 1a).

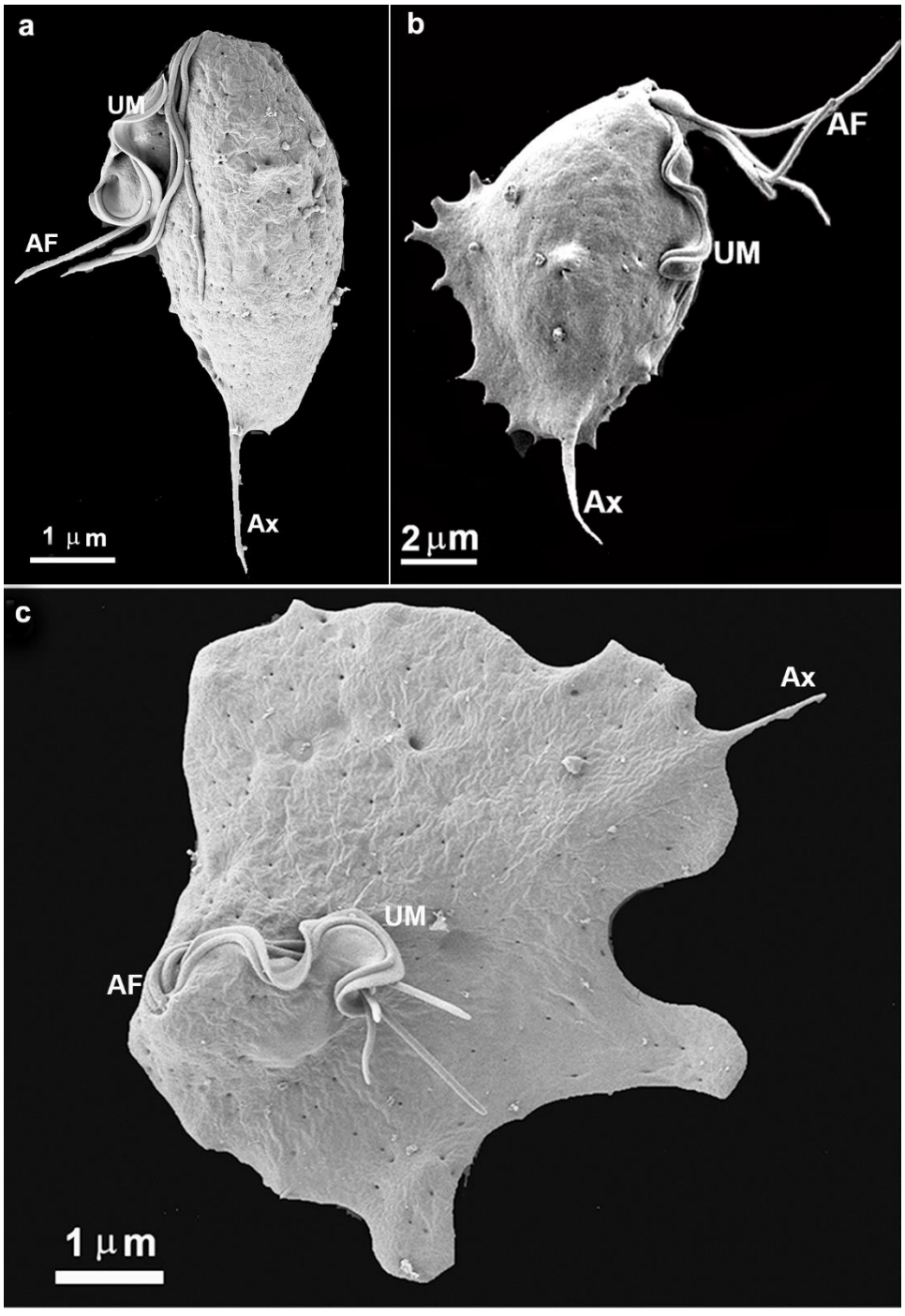

Figure 1. Scanning electron microscopy of the parasite *T. vaginalis* grown in axenic culture (a) and after contact with an inert substrate or host cell (b-c). (b) A cell was taken almost immediately after adhesion to the flask bottom. Notice that small cell surface projections are seen, which do not occur in free cells. AF, anterior flagella; Ax, axostyle; UM, undulating membrane.

We observed a gradual contact between single cells with the bottom flask in all experimental assays. In a few seconds, the parasite emits cell surface projections such as filopodia, lamellipodia, and pseudopods (Figs. 1b, 2a, 2b,2c). The cells were so firmly adhered to the bottom flask that even

Preprints (www.preprints.org) | NOT PEER-REVIEWED | Posted: 3 October 2023 doi:10.20944/preprints202309.2050.v1

several washes did not remove them. One interesting observation was that the undulating membrane was expanded and did not participate in the neighboring cells' contact (Fig. 2b). The flagella touched a neighboring cell and thus seemed to participate in cell recognition and approaching the two cells (Fig. 2e).

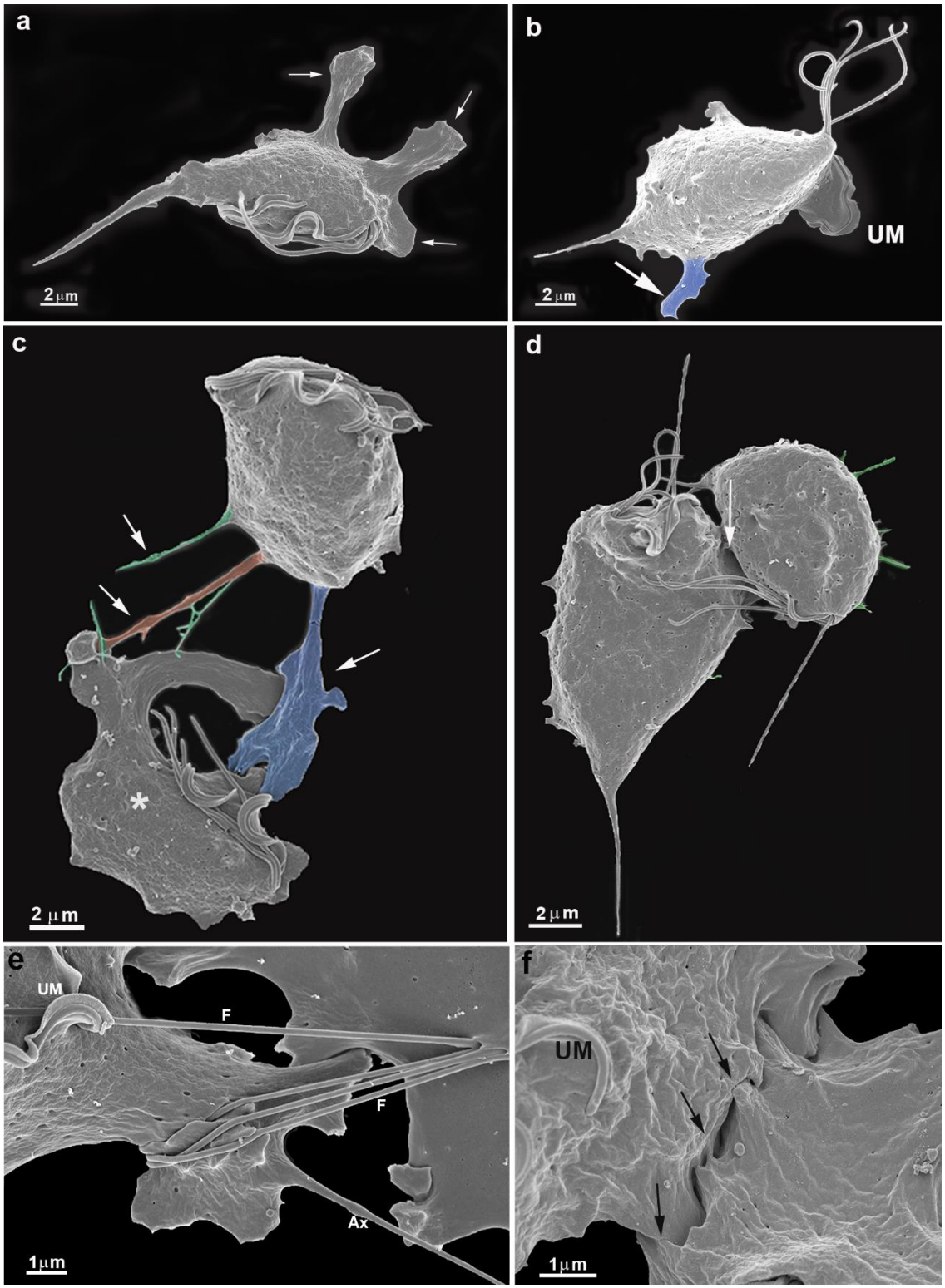

Figure 2. Scanning electron microscopy of *T. vaginalis* collected from the flask bottom after a few minutes of cultivation. Parasites were fixed in situ, washed several times, and processed for SEM. Notice large cell projections in blue (a-c), filopodia (orange), and cytonemes (green). (c-d) Early contacts between two parasites (arrows). Notice cell projections and changes in the shape of one cell

Preprints (www.preprints.org) | NOT PEER-REVIEWED | Posted: 3 October 2023 doi:10.20944/preprints202309.2050.v1

(c, asterisk). (e-f) Cells in contact. Notice the flagella contacts with a neighboring cell (e) and close contacts between cell surfaces (f). UM, undulating membrane.

Cells' contacts progressed from two next to three, four, and five (Figs. 2c-f; 3a-b). Points of contact between plasma membranes are observed (Figs. 2d, 2f, 4).

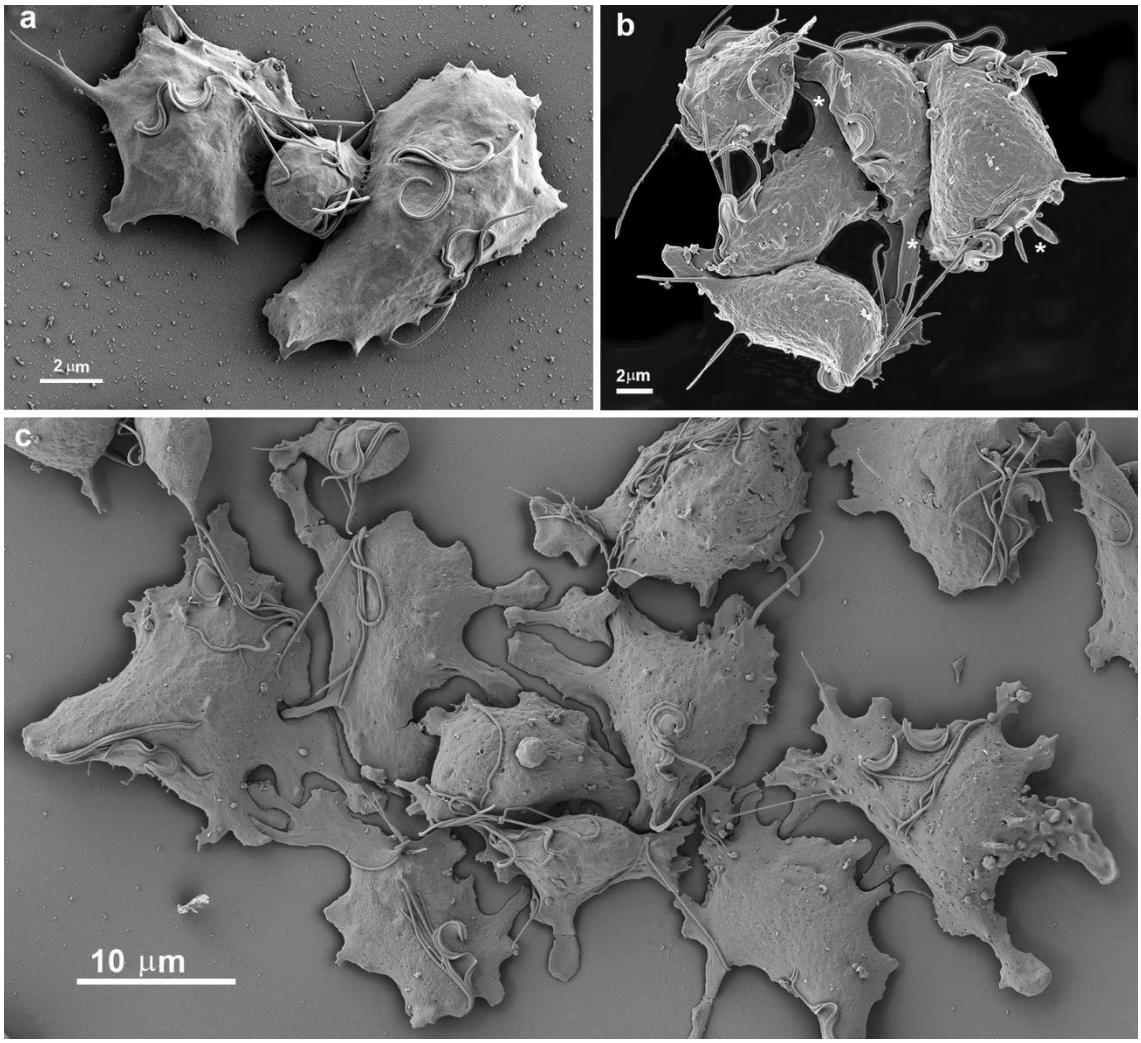

Figure 3. Scanning electron microscopy of *T. vaginalis* adhered to flask bottom (a, c) and under cluster formation (b). (a, c) A monolayer in the process of formation. The cells are becoming flattened, and flagella are always free. (b) A cluster of five cells. Notice surface projections (asterisks).

Preprints (www.preprints.org) | NOT PEER-REVIEWED | Posted: 3 October 2023 doi:10.20944/preprints202309.2050.v1

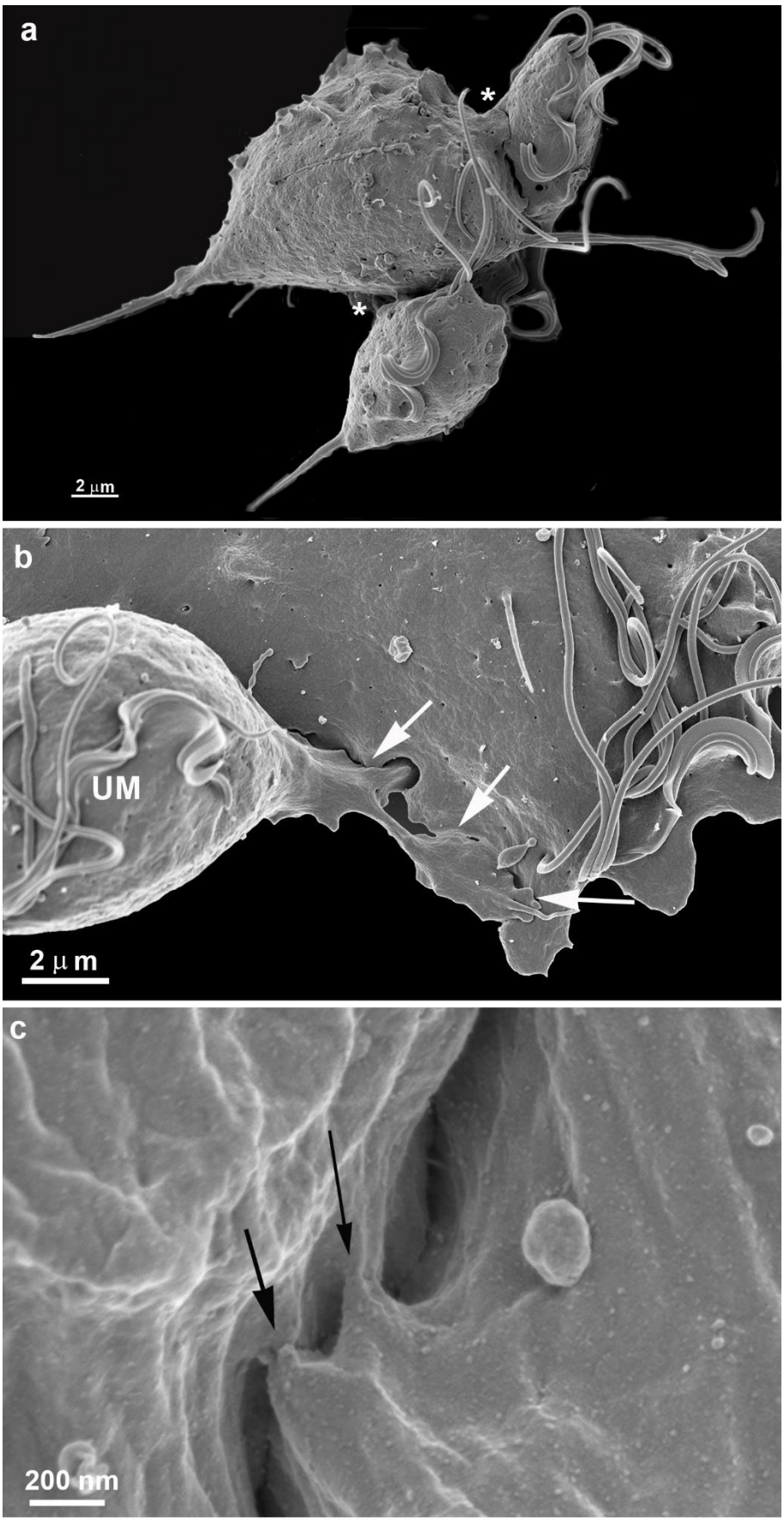

Figure 4. Scanning electron microscopy of *T. vaginalis* during two different situations. In (a), at the beginning of cluster formation, b-c cells adhered to the inert substrate. (a) Three cells are in tight

 doi:10.20944/preprints202309.2050.v1

contact (asterisks). Notice that the flagella are free. (b-c) Contact points between cells are observed (arrows). UM, undulating membrane.

More cells gradually come close, adhere, and form a monolayer (Figs. 3c, 5-7). It is important to mention that a second layer of parasites adheres when the monolayer is formed (Figs. 4b, 11). We tested different strains with low and high virulence, and all formed monolayers when in contact with the flask bottom. The analyses were made using light, scanning (SEM), and transmission electron microscopy (TEM) (Figs 5-13). The adhesion between the cells was strong, and the cells did not separate when the monolayer was scrapped from the flask. It was not necessary to add host cells to induce monolayer formation. Observing the samples with SEM revealed that the parasites were pear-shaped in the first moment. However, they become gradually ameboid, flattened, and spread over the inert surface (Figs. 2-5). During monolayer formation, all flagella are kept upward and never in contact with the flask bottom (Figs. 2-5).

Preprints (www.preprints.org) | NOT PEER-REVIEWED | Posted: 3 October 2023 doi:10.20944/preprints202309.2050.v1

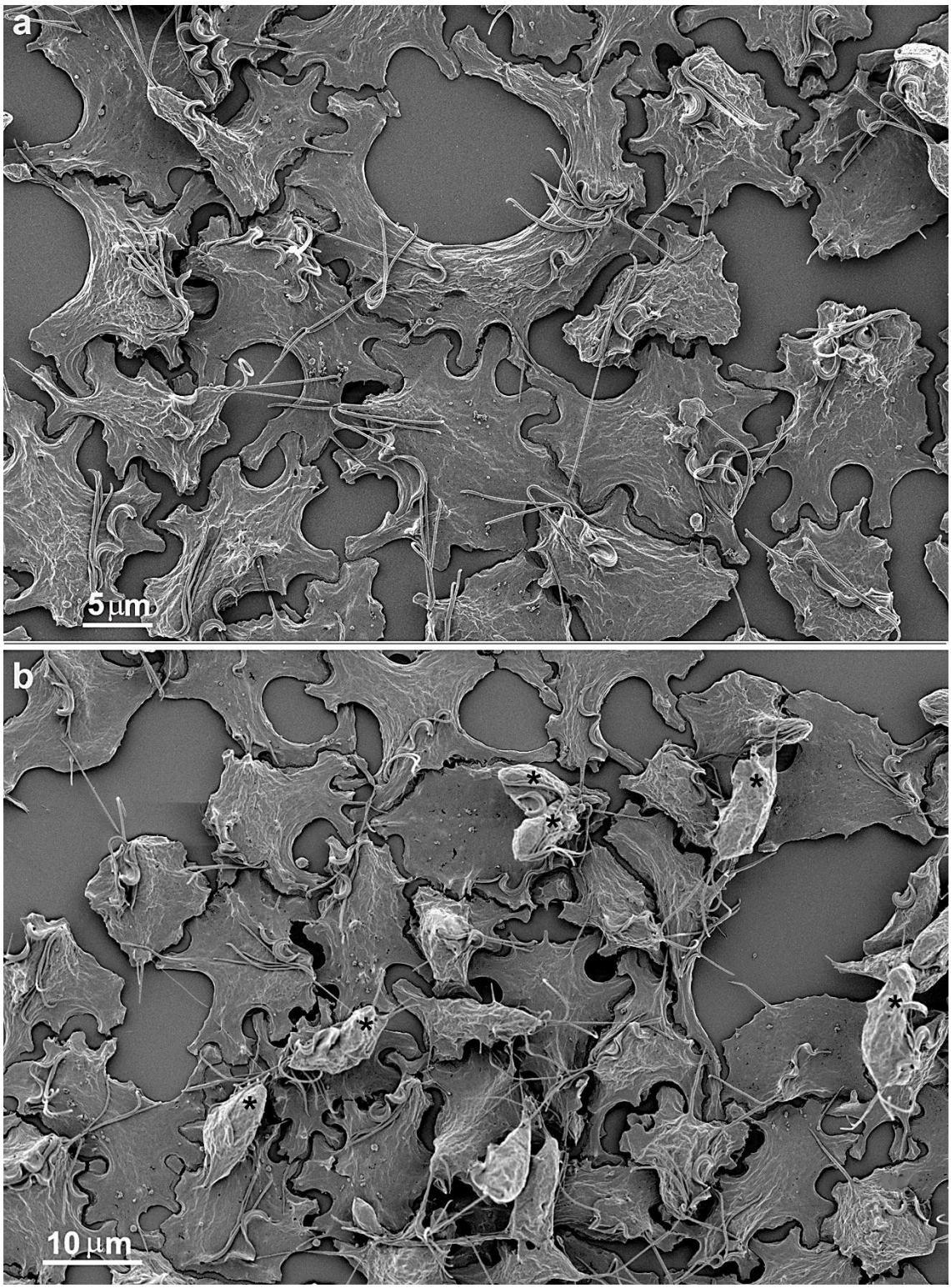

Figure 5. Scanning electron microscopy of *T. vaginalis* forming a monolayer. Notice the flattened parasites presenting cell contacts with the neighbors. In (b), a second layer of parasites is in the adhesion process (asterisks).

Preprints (www.preprints.org) | NOT PEER-REVIEWED | Posted: 3 October 2023 doi:10.20944/preprints202309.2050.v1

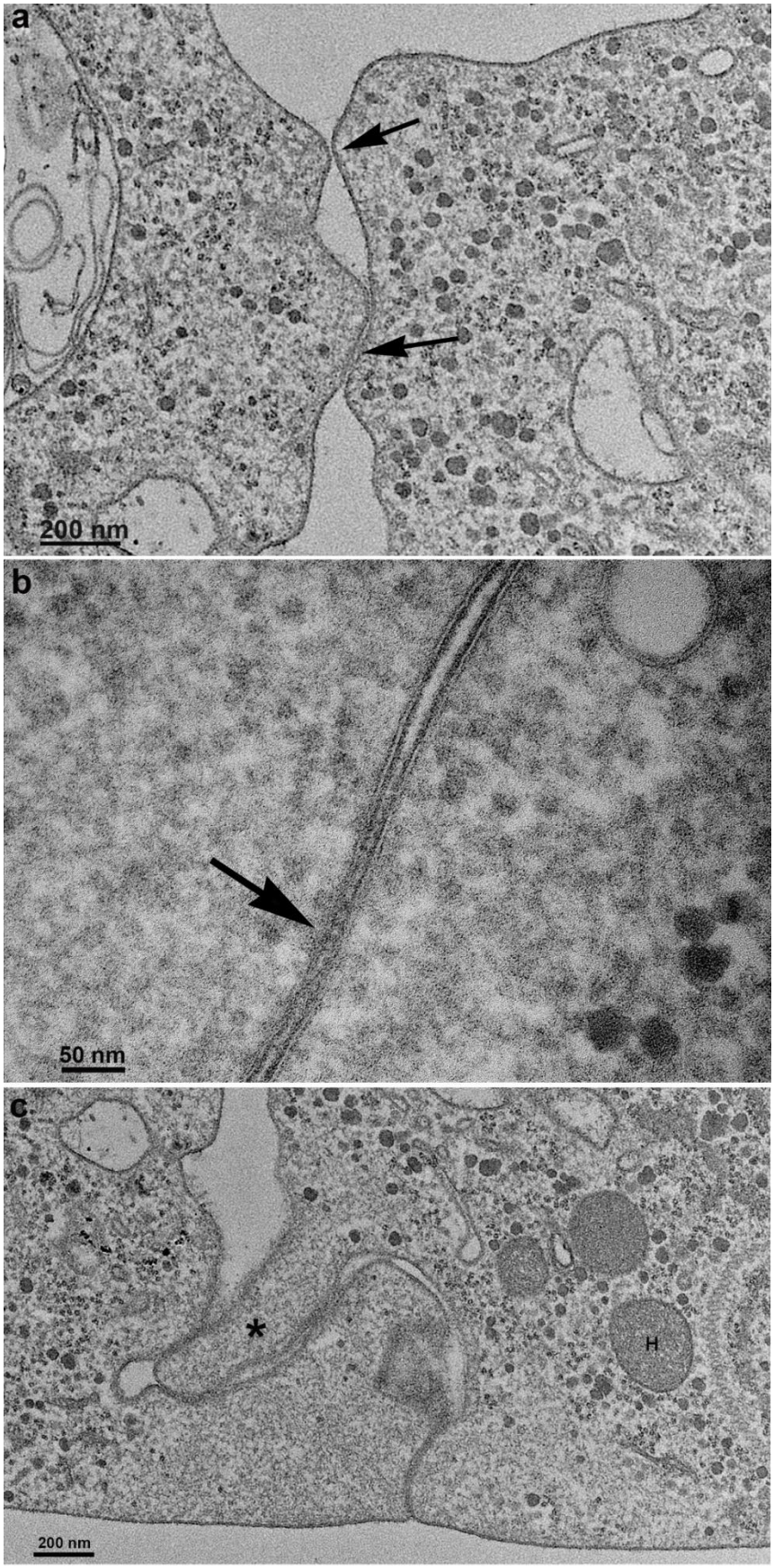

Figure 6. TEM of sequential images of the first *T. vaginalis* cell contacts until the formation of the monolayer on the flask bottom. **(a-b)** Plasma membranes are in touch. Notice glycocalyx contacts. **(c)** Beginning of the formation of the first interdigitations (asterisk).

Preprints (www.preprints.org) | NOT PEER-REVIEWED | Posted: 3 October 2023 doi:10.20944/preprints202309.2050.v1

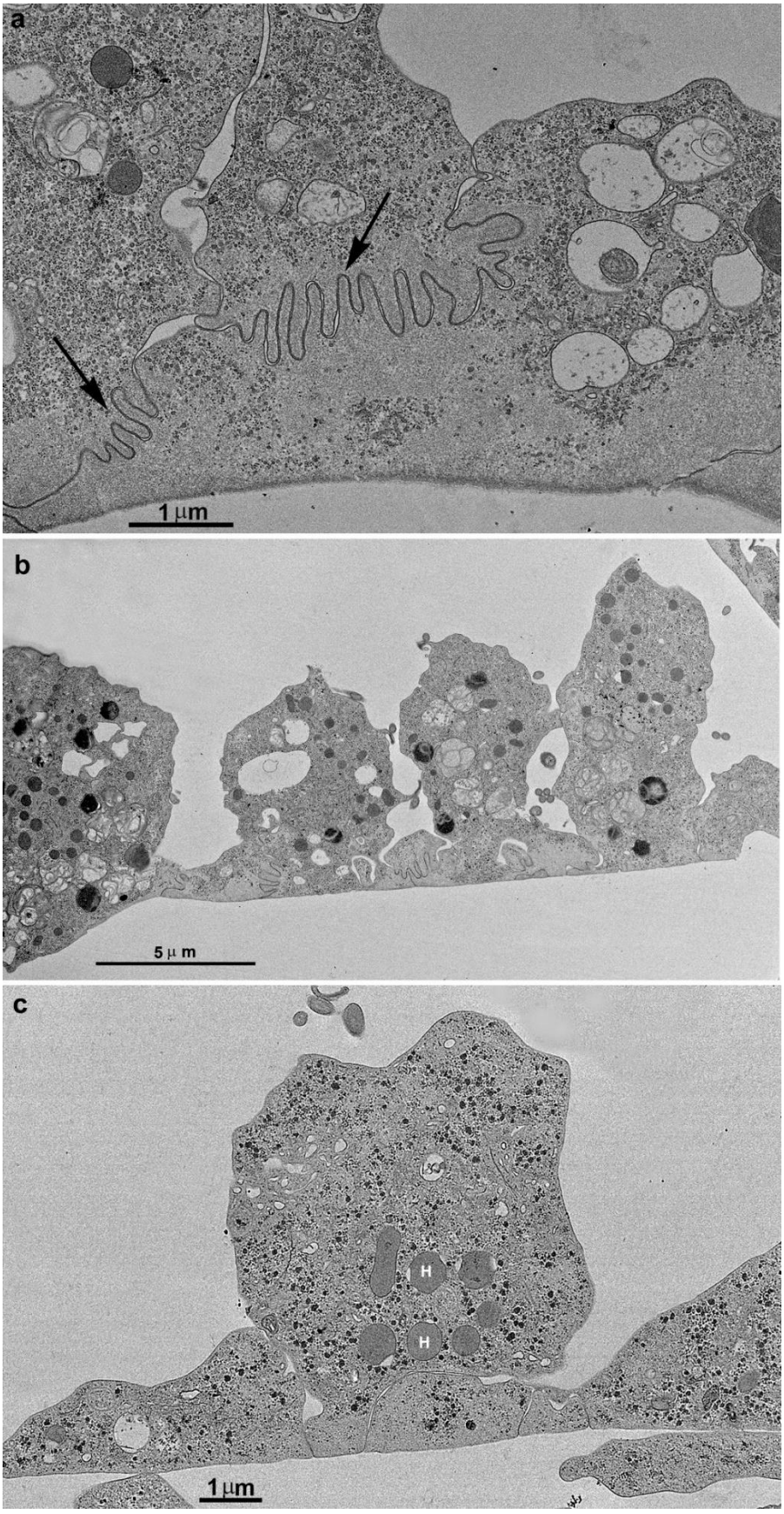

Figure 7. TEM of sequential images of the first *T. vaginalis* cell contacts until the formation of the monolayer on the flask bottom. **(a)** New and deep interdigitations form, promoting a strong bond between cells (arrows). Note that just below the cell surface is an area devoid of organelles. **(b-c)** The cells are already tightly bound together, forming a monolayer. H, hydrogenosomo.

Preprints (www.preprints.org) | NOT PEER-REVIEWED | Posted: 3 October 2023 doi:10.20944/preprints202309.2050.v1

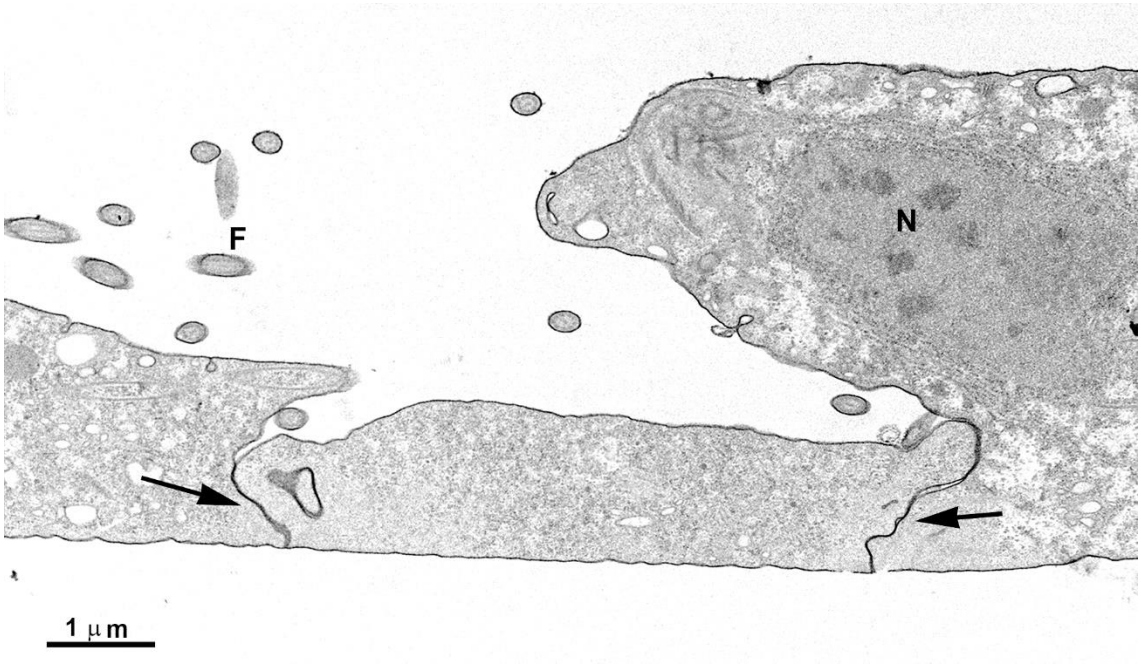

Figure 8. TEM of *T. vaginalis* incubated with ruthenium red and not stained with uranyl acetate. Notice that the parasites are adhered to the flask bottom, forming a monolayer. The arrows point to the contact between the plasma membranes, indicating that the stain could pass between the cells. F, flagella; N, nucleus.

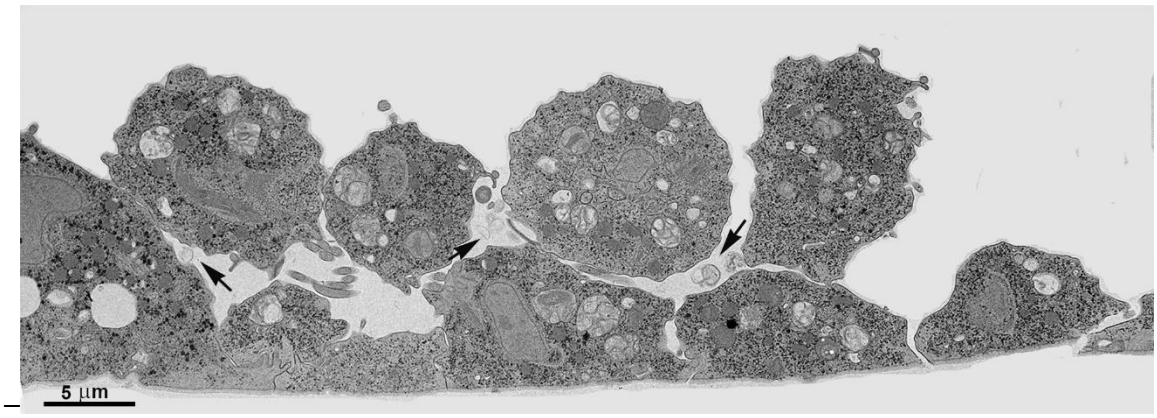

Figure 9. TEM of adhered parasites after incubation in a plastic flask. The first layer of cells is firmly adhered, forming many interdigitations. The second layer of cells exhibits cell contacts but without interdigitations. Notice the presence of multivesicular bodies in vesicles (V) inside the cells and also observed in the extracellular region (arrows).

When analyses were done in TEM, we could note the first observations of plasma membrane contacts, followed by several close contacts between the parasites. The membranes were very close in several images and appeared fused in some situations. Then, we used markers such as ruthenium red (Fig. 8) and the Thiéry technique (FIGs. 9-11) to check if there was membrane fusion and if there would be passage of molecules between the cell-cell contact areas. Furthermore, we obtained tomograms in regions with doubts about whether fusion would occur. In this way, thick slices of the interaction areas were aligned, and with a 120KV TEM acceleration, sequential and deep images were obtained. What appeared to be a fusion between cell membranes turned out to be cells with their membranes intact, without fusion occurring. Thus, no fusion between the cell membranes of the parasites forming the monolayer was seen (Fig. 10, SUPL. 1).

Preprints (www.preprints.org) | NOT PEER-REVIEWED | Posted: 3 October 2023 doi:10.20944/preprints202309.2050.v1

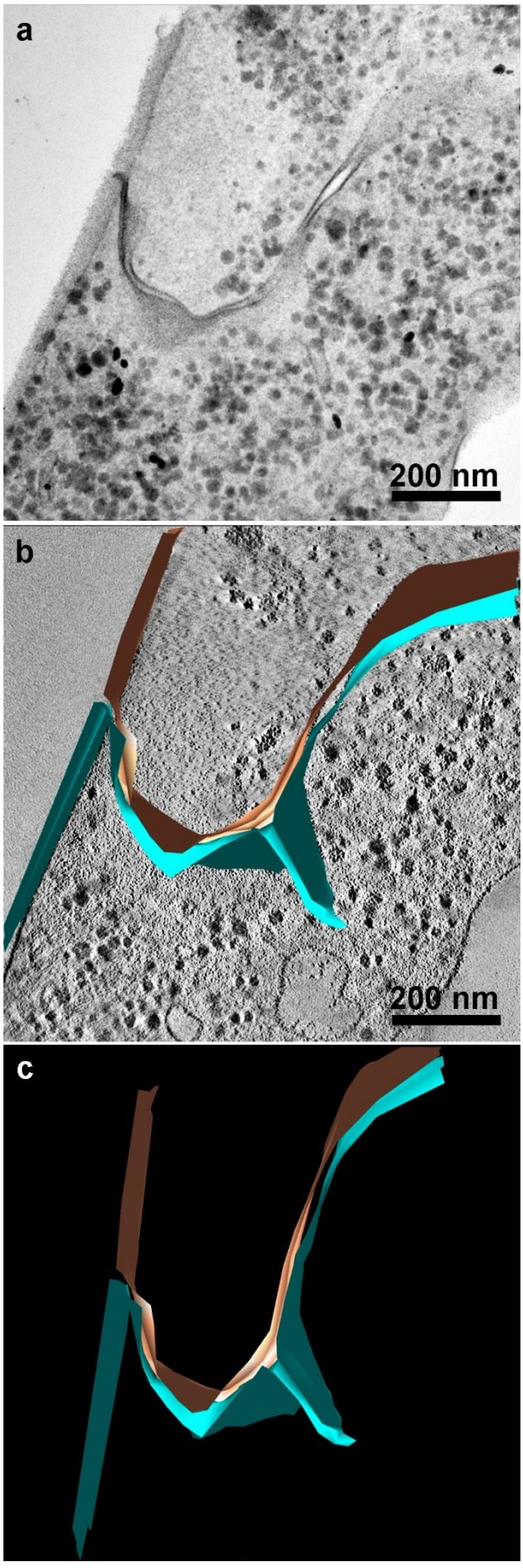

Preprints (www.preprints.org) | NOT PEER-REVIEWED | Posted: 3 October 2023 doi:10.20944/preprints202309.2050.v1

Figure 10. (a) Transmission electron microscopy of *T. vaginalis* in a region of two cells in contact in monolayer formation. (b) Virtual slices from a tomogram were obtained by TEM–tomography, where a closer region is reconstructed and colorized. (c) 3D model of the tomogram. The two plasma membranes are shown in brown and blue; no membrane fusion was noticed.

Extrusion of extracellular vesicles

During the monolayer formation, we observed the presence of extracellular vesicles in the extracellular environment, in close contact with other parasites. We also observed multivesicular bodies in the cells' internal vacuoles (Fig. 11). Interestingly, there were no host cells, only other parasites of the same strain (Figs. 9, 11).

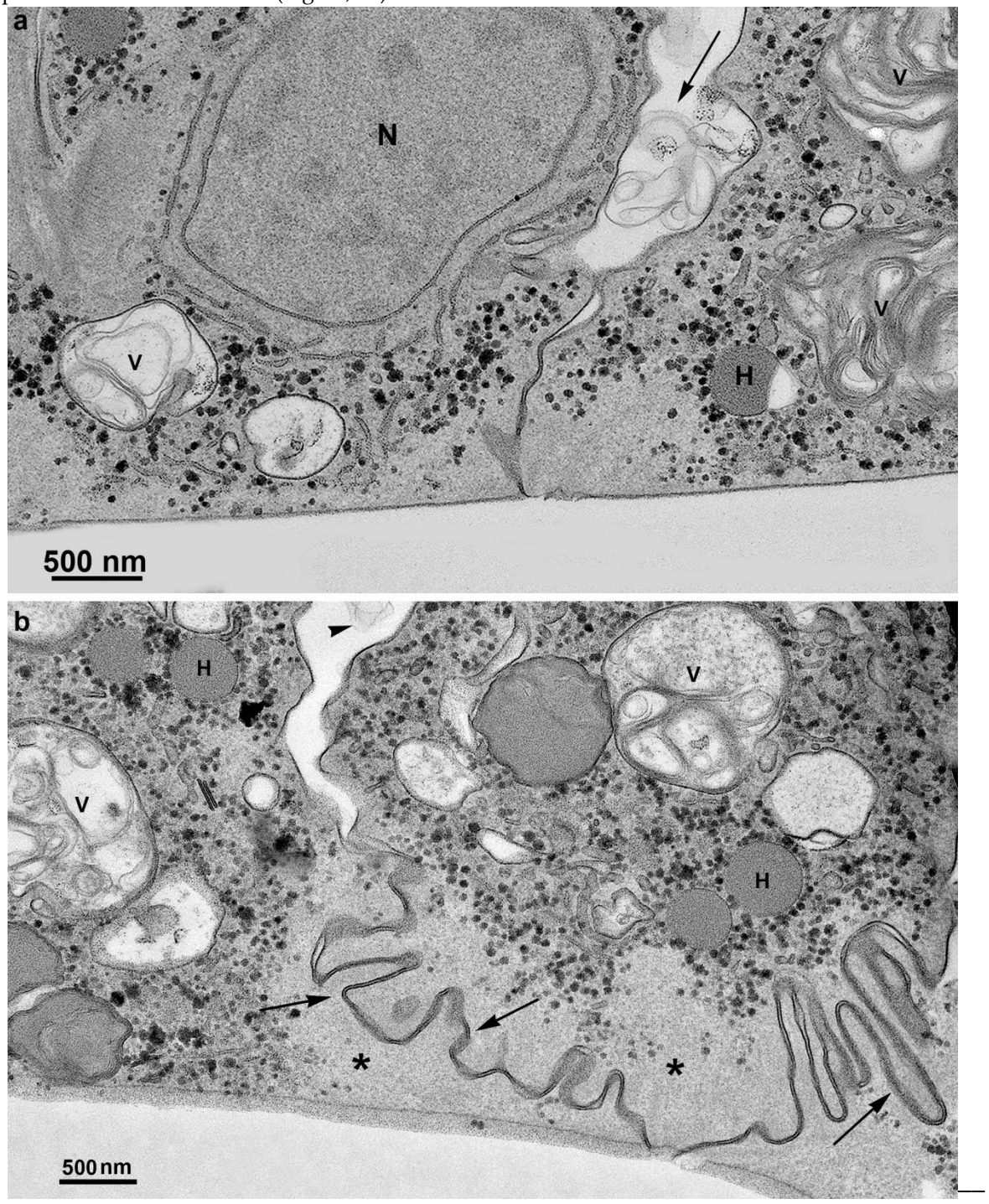

Figure 11. TEM of parasites in contact forming a monolayer after Thiéry technique that reveals carbohydrates. Notice positive reaction in glycogen granules (black dots) and cell membranes. Many

Preprints (www.preprints.org) | NOT PEER-REVIEWED | Posted: 3 October 2023 doi:10.20944/preprints202309.2050.v1

vesicles (V) containing multivesicular bodies are also observed in the extracellular region (arrows). In (b), notice the interdigitations (arrows) and the absence of organelles in the areas of cell contacts (asterisks). H, hydrogenosome.

3.2. Proteins of junctional areas

We also decided to look for known proteins present in junctional areas of cells that form epithelia in metazoan cells. We tested claudin, occludin, and ZO-1 with commercial antibodies. All gave negative results. Regarding tests with anti-cadherin antibodies, we started with a recent group publication [14], which found a protein similar to cadherin using bioinformatics. We used various commercial pan-cadherin antibodies. A positive reaction was observed, albeit not in cell-cell contact regions, but in the anterior portion near the communication interface between the cytoskeleton and the plasma membrane (Fig. 12). When we tested enriched fractions of *T. vaginalis* cytoskeleton after detergent-based extraction using anti-tubulin and anti-cadherin antibodies we noticed a colocalization of the labelings (Fig. 13) indicating a non-specificity of the commercial anti-cadherin antibodies.

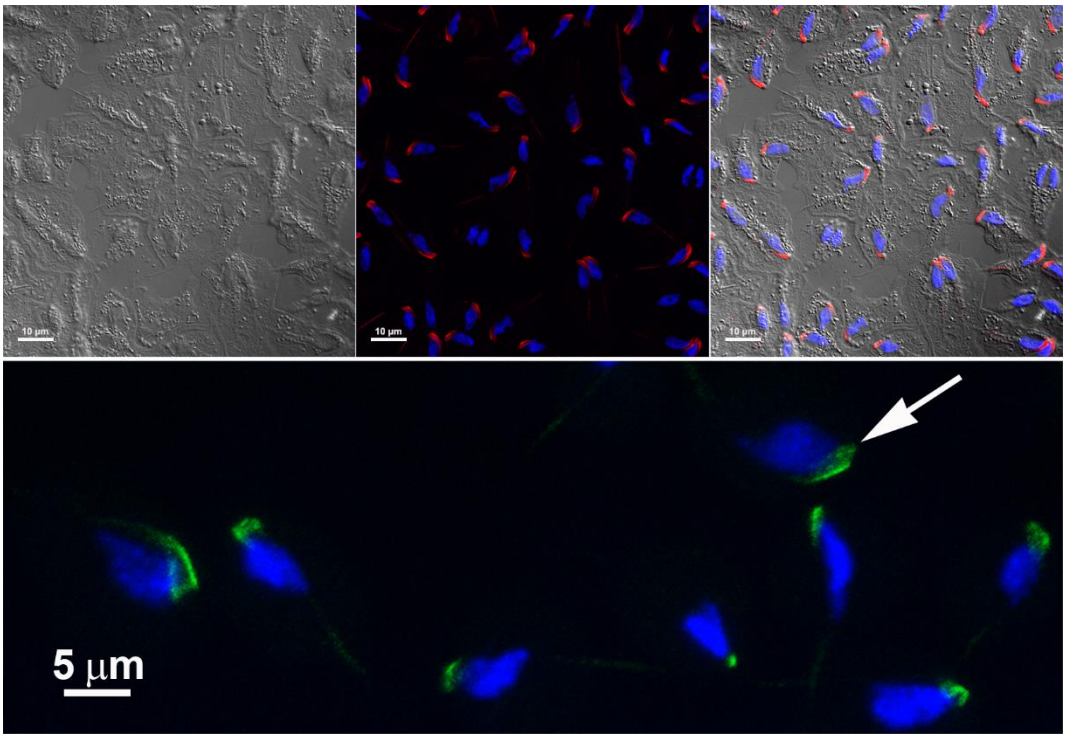

Figure 12. Immunofluorescence microscopy of *T. vaginalis* monolayer after labeling with an anti-E-cadherin polyclonal antibody (in red and green). The nuclei are stained with DAPI (blue). Notice that the anterior portion near the interface between the cytoskeleton and the plasma membrane is labeled with polyclonal anti-E-cadherin (arrow).

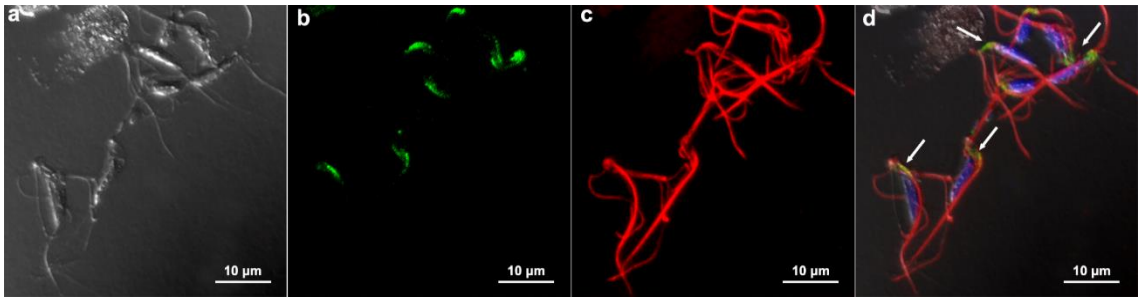

Figure 13. Enriched fraction of *T. vaginalis* cytoskeleton after detergent-based extraction. (a) Differential interference contrast microscopy; (b) immunofluorescence microscopy using an anti-E-

Preprints (www.preprints.org) | NOT PEER-REVIEWED | Posted: 3 October 2023 doi:10.20944/preprints202309.2050.v1

cadherin polyclonal antibody; (c) labeling with an anti-alpha-tubulin. In (d), note the colocalization of the labeling (white arrows). The nuclei are stained with DAPI (blue).

3.3. Communication between parasites

Intending to verify whether there was a passage of information between adjacent cells that formed the monolayer, as occurs in gap junctions, we proceeded with an experimental injection of the fluorescent dye Lucifer Yellow, which was injected in one cell, and pictures were taken 2 min later, searching whether the dye was found in neighboring cells. The results were negative. The dye was restricted to the injection site (Fig. 14).

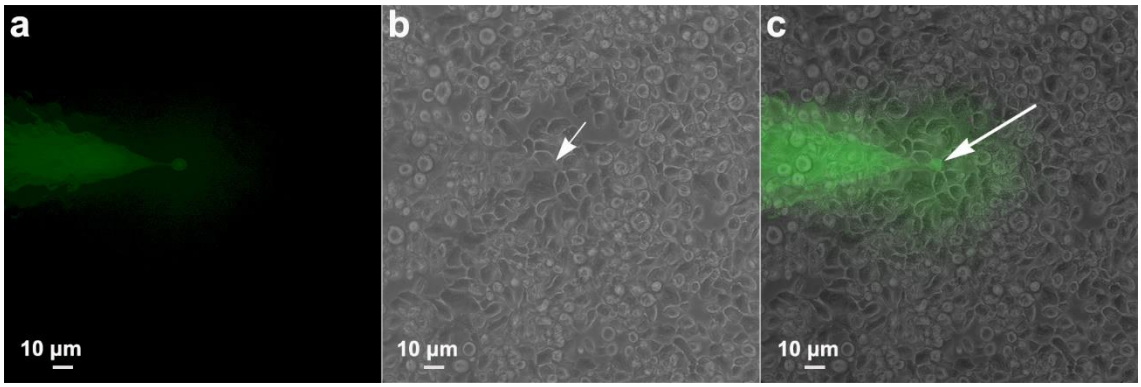

Figure 14. Functional analysis of a possible gap junction coupling among *T. vaginalis* monolayer. Lucifer Yellow was injected in one cell, and pictures were taken 2 min later. In (a) fluorescence, (b) phase contrast, and (c) merged. Notice that the dye remained restricted to the injected cell (arrow).

4. Cluster formation

While cultivating different strains of *T. vaginalis*, we observed the formation of cell aggregates that can reach hundreds of attached parasites (Figs. 15-16). It was noticed that the contacts occur without the formation of interdigitations, as in the formation of monolayers. Furthermore, the aggregates are fragile and disperse after vigorously shaking the tubes, which does not occur with monolayers when the parasites adhere to the tube walls with inert material.

Preprints (www.preprints.org) | NOT PEER-REVIEWED | Posted: 3 October 2023 doi:10.20944/preprints202309.2050.v1

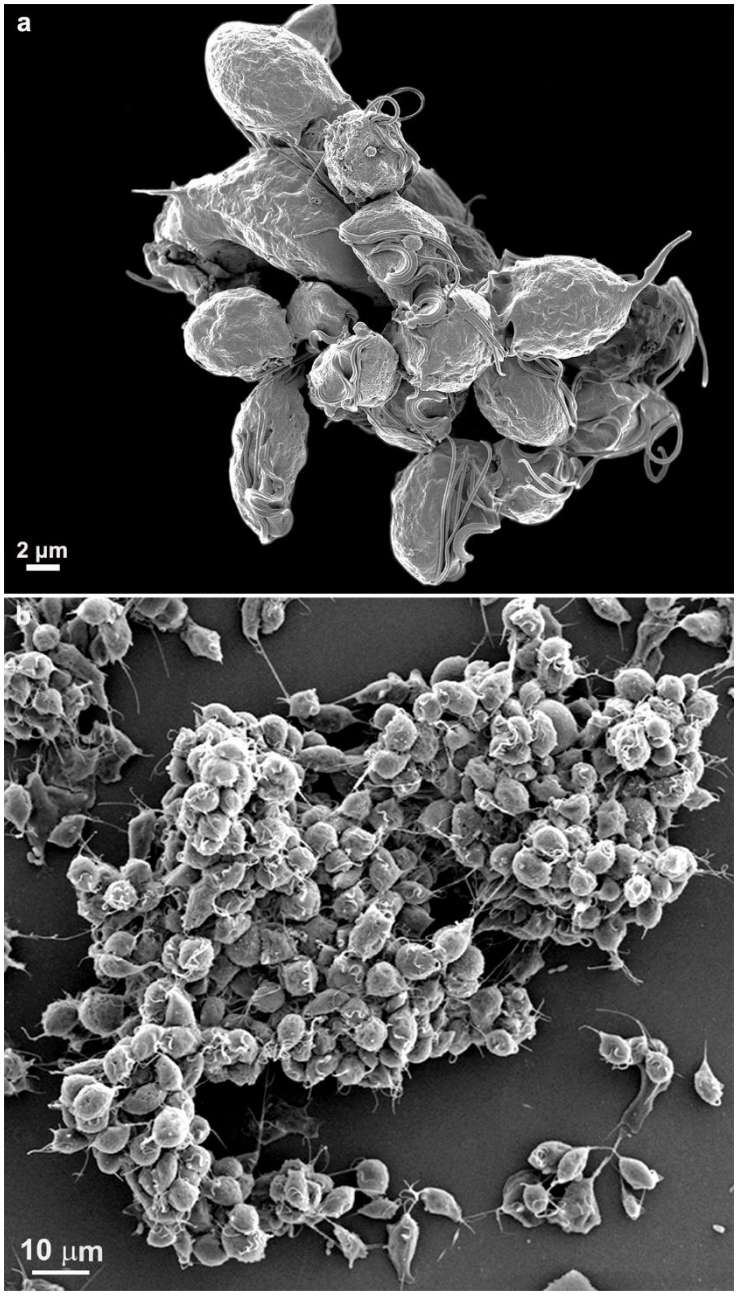

Figure 15. Scanning electron microscopy of SEM shows a large cluster formed by hundreds of *T. vaginalis*.

4.1. Transmission electron microscopy- First steps of clumping

Preprints (www.preprints.org) | NOT PEER-REVIEWED | Posted: 3 October 2023 doi:10.20944/preprints202309.2050.v1

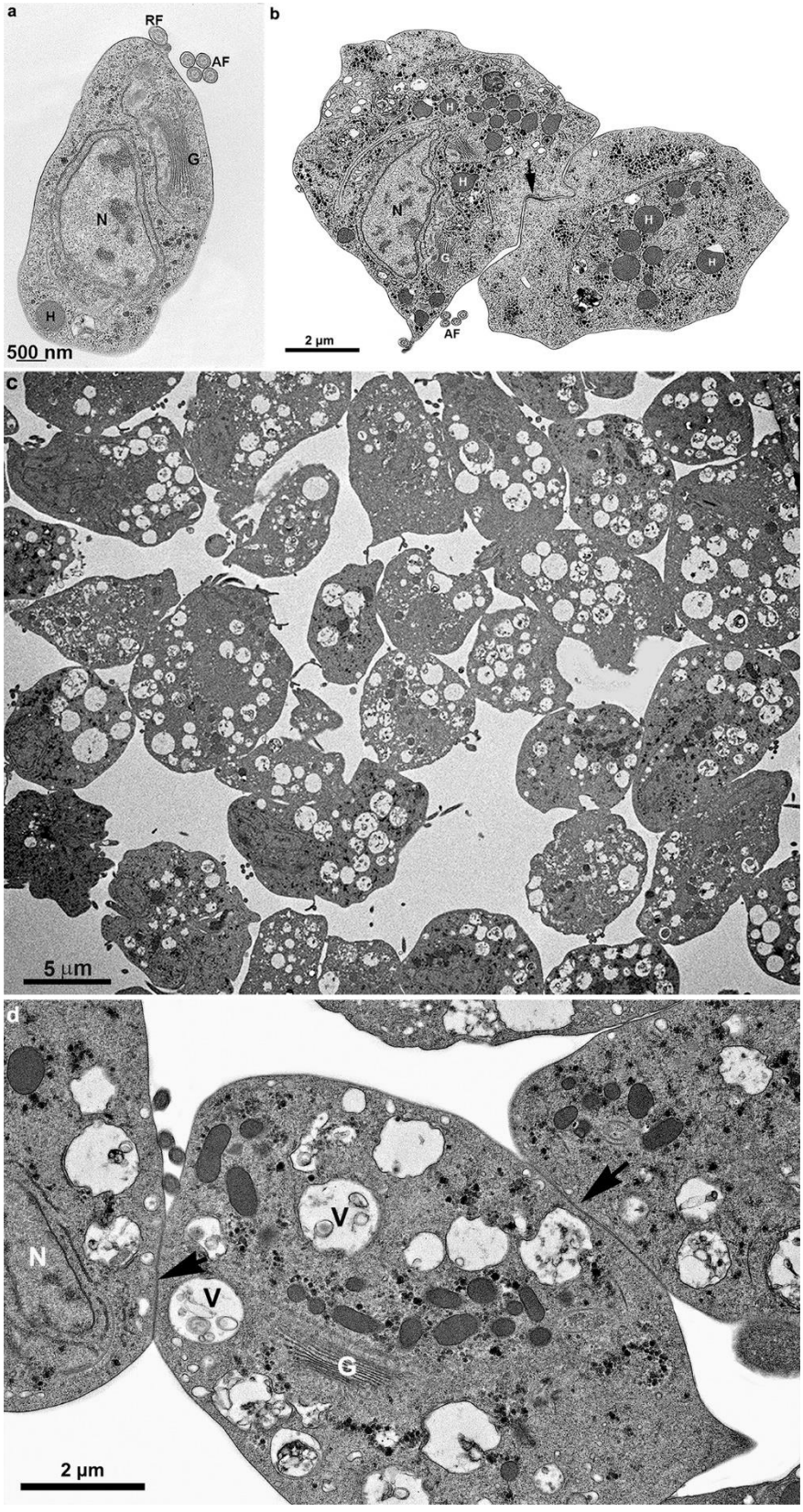

Figure 16. Transmission electron microscopy of *T. vaginalis* from the supernatant culture. Notice in (a) before contact with other cells, (b) early cell contact, and (c-d) after a cluster formation. The arrows point to a region of adhesion. AF, anterior flagella; G, Golgi; H, hydrogenosome; N, nucleus; RF, recurrent flagellum; V, vacuole with multivesicular bodies.

Discussion

 doi:10.20944/preprints202309.2050.v1

T. vaginalis is an extracellular parasite that uses adherence as a crucial factor for its pathogenicity. Many studies have reported molecules and factors indispensable for infection [15-16]. Those that analyze the behavior and mode of parasites adhering to one another are very important and help elucidate parasite survival and infection.

In the present work, we analyzed the formation of monolayers and parasite clusters using high-resolution scanning electron microscopy, among other techniques. Even though it was an inert material, the parasites came into contact with membranes and formed a uniform layer of tightly adherent cells, similar to an epithelium. Based on this observation, we proceeded to analyze whether (1) there would be a fusion between the cell membranes of the parasites, (2) there would be a passage of molecules between the contact areas, and (3) there would be a passage of molecules between the cells of the monolayer, as occurs in gap junctions. We used advanced microscopic analysis, such as high-resolution SEM and TEM immunostaining using antibodies against junctional area proteins found in epithelial cells, ultrastructural tomography, and fluorescent dye injection to check if parasite communication occurred.

5.1. Monolayer formation by T. vaginalis

It has been demonstrated in several works that *Trichomonas vaginalis* can adhere to plastic surfaces in the presence of various agents and under different experimental conditions [17-21]. In addition, one group [21] demonstrated that the parasite can adhere to polystyrene, intrauterine device, and vaginal ring. However, although another group [19] reported that actin was important in the adhesion of neighboring cells and showed some information, a detailed ultrastructural report has not been published. When comparing *T. vaginalis* adhesion to an inert substrate with the host cell, the authors have shown that high adhesin gene expression levels were observed only in trophozoites attached to the cells [22]. One study [20] compared the in vitro adhesion of *T. vaginalis* to plastic, testing parent and lipophosphoglycan (LPG) mutants, and showed that they differed in attachment to plastic surfaces.

5.2. Clumping

The observation of clumps has already been reported in some previous articles, suggesting that aggregation may have a role in the pathology of *Trichomonas* [8,10,14]. However, the importance of clumping and the stages of clump formation and cell-to-cell union under morphological aspects had not yet been described. Previous works defined a clump as an aggregate of ~10 or more parasites [10,14]. Here, using electron microscopy, it was possible to see that hundreds of parasites can form a clump. We observed that the first clumps are easily disrupted by pipetting, indicating a fragile adhesion, which differed from the observation on monolayers, firmly adhered.

It has been reported that cytonemes are associated with clump formation [23] and that highly adherent strains aggregate more than poorly adherent strains [10,23-24]. The authors demonstrated that different parasites inside the clumps are connected by cytonemes, which are longer filopodia extensions reaching up to ~300 nm from the originating cell body [23]. The authors reported that interaction between different strains induced cytoneme formation [25] and that parasite clumping is strain-dependent. In addition, the size-variable microcolonies dysregulate epithelium permeability or promote its destruction. However, the authors did not show references for these disease facts, although it was not a full paper but a parasite comment of the month. In addition, the authors reported that different *T. vaginalis* strains communicated through cytoneme-like membranous cell connections, and the cytoneme formation of an adherent parasite strain is affected in the presence of a different strain [23]. In our work, filopodia and cytonemes are longer than 6 μm, and we showed no need for different strains to form filopodia, cytonemes, and extracellular vesicles.

Several works have reported the transition from pear-shaped parasite to amoeboid, including the actin-based machinery and parasite migration across host tissue [19, 26]. One group [8] reported that axenic trophozoites clumped within the first 15 min of contact after adhering to target cells and transformed into an ameboid shape. However, the authors did not focus on the monolayer formation and the parasite's adhesion to inert substrates.

 doi:10.20944/preprints202309.2050.v1

Defining the molecules and the morphological characteristics that *T. vaginalis* uses may help us understand how the parasite colonizes the urogenital tract and how to prevent or treat infections.

Some authors have described the importance of the virulence of the strain [10,14,25] as a determining factor for the formation of clumps, indicating that calcium is also an important ion for that. In the present work, we did not verify these indications. All strains analyzed showed clumps, regardless of whether they had high or low virulence. However, the strains we used were different from the other groups.

Pachano group [9] reported that increased histone acetylation leads to increased parasite aggregation and adherence to host cells. The authors claimed that TSA treatment is responsible, at least partly, for increased parasite clumping and adhesion of the parasite to human host cells. In addition, Coceres et al., 2015 [10] showed that increased TSP8 expression increased parasite aggregation in TSA-treated parasites.

Recently, epigenetic regulation for *T. vaginalis* cytoadherence and parasite aggregation has been proposed [21]. The authors reported that when a less-adherent strain was treated with the histone deacetylase inhibitor trichostatin A (TSA), cytoadherence and parasite aggregation were improved, supporting this observation's relevance. In addition, galectins binding *T. vaginalis* surface lipoglycans have been reported as one of the potential factors triggering parasite swarming [27]. Thus, one group [21] applied lactose to compete with the interaction between galectin and the parasite ligand. The authors observed that the parasite clusters on host cells were significantly reduced, indicating that lactose could compete with parasite aggregation.

Although it has been reported that clumping does not occur in all parasite strains, here we found that adhesion cell-to-cell to form an adhesive parasite monolayer occurred in all strains so far examined by us. As far as we know, this is the first study showing that *T. vaginalis* forms a very tight monolayer before clumping when in contact with an inert substrate.

The association of clumping with parasite adherence is interesting in light of emerging evidence suggesting that aggregation may have a role in the pathology of *Trichomonas*. Defining the biochemical properties required for adhesive phenotypes of *T. vaginalis* may help us understand how the parasite colonizes the urogenital tract and how to prevent or treat infections.

5.3. E-cadherin

A previous bioinformatic work [14] characterized a hypothetical protein, TVAG_393390, which was renamed cadherin-like protein (CLP). Its predicted tertiary structure was similar to mammalian cadherin proteins involved in cell-cell adherence. The authors showed that *T. vaginalis* overexpressing CLP has ~a 3.5-fold greater adherence to host cells. These analyses described the first parasitic CLP.

In addition, one group [14] showed that adding Ca^2 but not the presence of host cells significantly increased the clumping of parasites. These data together suggest that parasite clumping is calcium-dependent. In our work, we observed that calcium did not interfere in monolayer formation. The fact that we have used inert flaks indicated that the ability to form clumps and monolayers does not necessitate a host signal.

Because cadherin proteins are conserved metazoan proteins with important participation in cell-cell adhesion, and the Chen group [14] claimed that cadherin-like protein is more abundant on the surface of parasites and mediates parasite-parasite and parasite-host adherence, we decided to analyze the presence of cadherins on the region of cell-cell contact, in the trichomonads monolayers observed in the present study.

Our analyses were made using immunolabeling commercial pan-cadherin antibodies and analyzed with immunofluorescence and transmission electron microscopy. We used anti-cadherin antibodies from different sources, and the essays were repeated several times. We only found a positive reaction in the anterior portion near the interface between the cytoskeleton and the plasma membrane using the antibody anti-E-cadherin polyclonal antibody (Invitrogen, PA5-32178). Still, no labeling was observed on the parasite cell surface or in the cell-cell contact region.

 doi:10.20944/preprints202309.2050.v1

We investigated the potential proteins that were labeled with this antibody. We employed the TrichDB BLAST tool to compare the peptide sequence of the commercial E-cadherin Polyclonal Antibody with the *T. vaginalis* genome. We identified the protein TVAGG3_0955330 as the best match, scoring 31.6 and an E-value of 0.62. It was described as an 'ankyrin repeat protein family,' and computationally inferred from orthology, its predicted function is the transfer of phosphorus-containing groups. Ankyrins mediate the attachment of integral membrane proteins to the spectrin-actin-based membrane cytoskeleton [28,29]. Following detergent treatment, we performed immunofluorescence assays on fixed whole cells, live cells, and isolated cytoskeletons. We labeled with a monoclonal anti-alpha-tubulin (TAT-1, kindly donated by Dr. Keith Gull) to identify the cytoskeleton and check the localization with the labeling with E-cadherin polyclonal antibody.

It is important to point out that the work of the Chen group [14] only found structural similarity with cadherins and that it is located in the cell membrane only when CLP was overexpressed, so it is difficult to say that it participates in communication between cells, since we have a vision of something more structural, where this protein localizes in cells without gene editing.

5.4. Interdigitations

In the present work, we observed that when parasites formed monolayers, extended areas in neighboring cells were tightly attached by multiple interdigitations of the adjacent cells. Flat ridges of neighboring cells are intensely interlocked, and the intercellular spaces are closed.

In metazoa, cell junctions of different types are responsible for several functions, such as mechanical, chemical, and electrical coupling of cells and forming particular barriers in epithelia and endothelia.

In the small intestinal epithelium extended areas, neighboring cells are tightly attached, and the epithelium is stabilized additionally by multiple interdigitations of the adjacent cells. In kidney tubules, these interdigitations are characterized by an extracellular space of relatively constant width (about 50 nm), separating the parallel membranes of adjacent cells.

Although single-celled eukaryotes, such as *T. vaginalis*, do not contain cell junctions, we demonstrated the formation of cell-cell junctional regions represented by interdigitations, similar to metazoa epithelia in parasites when in contact with an inert substrate. Previous work also reported the presence of interdigitations between parasites when in contact with host cells [8].

Here, we show that a protist, *T. vaginalis,* can establish a monolayer, similar to metazoa epithelia, concerning a tight adhesion between cells by interdigitations, providing a significant role in parasite attachment to and lysis of host cells. The monolayer and clusters of parasites would provide great resistance and stability since several cells can press the host cell with greater intensity, favoring the parasites as they could cause greater damage to the vaginal epithelium. In addition, the increased parasite-parasite association may further increase the number of parasites attacking the host cells.

One group [10] claimed that TvTSP8 from the Tetraspanin family (TvTSPs) was involved in parasite aggregation, suggesting a role for this protein in parasite: parasite interaction.

5.5. Extracellular vesicles

The presence of vesicular bodies has attracted much research interest, mainly in studies of interactions between parasites and hosts. The production of vesicles of different sizes has been demonstrated when *T. vaginalis* comes into contact with the host cell and when different strains are in contact, which has indicated changes in parasite adherence mediated by extracellular vesicles [16,23,24,30-32]. In addition, *T. vaginalis* exosomes modulate host immune responses since they induce an IL6 response in vaginal epithelial cells and downregulate the IL8 response to parasites [30].

T. vaginalis EVs have a diverse genetic material composition, primarily enriched with small RNAs. It has been suggested that they could modulate gene expression in recipient cells, potentially impacting parasite-parasite or parasite-host interactions. The delivery of these small RNAs to host cells for gene activity modulation is a promising area for further research [30,33].

EVs' presence and role in *T. vaginalis* when clumping during host interaction have not been deeply analyzed, and their participation in the infection process is still scarce. In the present study,

we observed the presence of large intracellular vacuoles containing multivesicular bodies and also the presence of extracellular vesicles. In the present case, there was no interaction with cells from different strains nor contact with a host cell. We observed an intense production of vesicles in sites of strong adhesion between the parasites. We suggest that microvesicles may also play a role in modulating information between parasites of the same strain, possibly exchanging important information about adherence between parasites. Thus, this is an important aspect that previous works have not pointed to. The parasites exchange pieces of information and appear to exchange information among themselves, even in the absence of other strains or host cells. It could occur by eliminating microvesicles after contact between the flagella or the cell membranes of two or more parasites. In our assays, we observed that any inert material entering the culture tube produces a strong reaction from trichomonas; for example, when a needle is introduced into the culture tube, the parasites immediately adhere to it. It leads us to suggest that the parasites seem to be programmed to be edacious for any material that serves as support and contact, thus being able to trigger their mechanism of adhesion or attack on homologous or foreign cells or even inert materials.

6. Conclusions

In conclusion, *T. vaginalis* behaves differently when clumping and when adhered to a substrate, where cells assume an ameboid shape and interdigitations firmly attach them and form a monolayer. In contrast, the clusters exhibit distinct plasma membrane contacts with no interdigitations, float in the cell cultures, and have fragile connections. In contrast, the monolayers are tightly adhered and do not separate even with high-speed centrifugation. Here, we also report that in the monolayer and cluster formation, no fusion or passage of molecules occurs in both events. In addition, our work shows no need for different strains to form filopodia, cytonemes, and extracellular vesicles during cluster formation. Extracellular vesicles were noted inside vacuoles and in the extracellular space in cells that adhered to the substrate and several filopodia in the parasite clusters.

Supplementary Materials: The following supporting information can be downloaded at the website of this paper posted on Preprints.org. Figure S1: title; Table S1: title; Video S1: title.

Author Contributions: Conceptualization, MB and FF; methodology, MB, FF, SO, RV.; validation, MB, FF; formal analysis, MB, FF, SO; RV; investigation, MB, SO, RV, FF; resources, MB.; data curation, MB, SO; writing—original draft preparation, MB.; writing—review and editing, MB.; visualization, MB, FF, SO; supervision, MB.; project administration, MB.; funding acquisition, MB. All authors have read and agreed to the published version of the manuscript.

Funding: This research was funded by Conselho Nacional de Desenvolvimento Científico e Tecnológico-CNPq, Fundação Carlos Chagas Filho de Amparo à Pesquisa do Estado do Rio de Janeiro (GRANT number E-26/200.956/2021), and FUNADESP.

Data Availability Statement: The data presented in this study are available on request from the corresponding author.

Acknowledgments: We thank Dr. Keith Gull (Sir William Dunn School of Pathology, University of Oxford, UK) for kindly providing the TAT-1 antibody.

Conflicts of Interest: The authors declare no conflict of interest.

References

1. Petrin, D.; Delgaty, K.; Bhatt, R.; Garber, G. Clinical and microbiological aspects of *Trichomonas vaginalis*. *Clin Microbiol Rev* **1998**, *11*, 300-317, doi:10.1128/cmr.11.2.300.
2. Sutcliffe, S.; Giovannucci, E.; Alderete, J.F.; Chang, T.H.; Gaydos, C.A.; Zenilman, J.M.; De Marzo, A.M.; Willett, W.C.; Platz, E.A. Plasma antibodies against *Trichomonas vaginalis* and subsequent risk of prostate cancer. *Cancer Epidemiol Biomarkers Prev* **2006**, *15*, 939-945, doi:10.1158/1055-9965.Epi-05-0781.
3. Maritz, J.M.; Land, KM; Carlton, J.M.; Hirt, R.P. What is the importance of zoonotic trichomonads for human health? *Trends Parasitol* **2014**, *30*, 333-341, doi:10.1016/j.pt.2014.05.005.

4. McLaren, L.C.; Davis, L.E.; Healy, G.R.; James, C.G. Isolation of *Trichomonas vaginalis* from the respiratory tract of infants with respiratory disease. *Pediatrics* **1983**, *71*, 888-890.
5. Van Der Pol, B.; Kwok, C.; Pierre-Louis, B.; Rinaldi, A.; Salata, R.A.; Chen, P.-L.; van de Wijgert, J.; Mmiro, F.; Mugerwa, R.; Chipato, T.; et al. *Trichomonas vaginalis* Infection and Human Immunodeficiency Virus Acquisition in African Women. *J. Infect Dis* **2008**, *197*, 548-554, doi:10.1086/526496.
6. Diamond, L.S. The establishment of various trichomonads of animals and man in axenic cultures. *J Parasitol* **1957**, *43*, 488-490.
7. Midlej, V.; Benchimol, M. *Trichomonas vaginalis* kills and eats--evidence for phagocytic activity as a cytopathic effect. *Parasitology* **2010**, *137*, 65-76, doi:10.1017/s0031182009991041.
8. González-Robles, A.; Lázaro-Haller, A.; Espinosa-Cantellano, M.; Anaya-Velázquez, F.; Martínez-Palomo, A. *Trichomonas vaginalis*: ultrastructural bases of the cytopathic effect. *J Eukaryot Microbiol* **1995**, *42*, 641-651, doi:10.1111/j.1550-7408.1995.tb05921.x.
9. Pachano, T.; Nievas, YR; Lizarraga, A.; Johnson, P.J.; Strobl-Mazzulla, P.H.; de Miguel, N. Epigenetics regulates transcription and pathogenesis in the parasite *Trichomonas vaginalis*. *Cell Microbiol* **2017**, *19*, doi:10.1111/cmi.12716.
10. Coceres, V.M.; Alonso, A.M.; Nievas, Y.R.; Midlej, V.; Frontera, L.; Benchimol, M.; Johnson, P.J.; de Miguel, N. The C-terminal tail of tetraspanin proteins regulates their intracellular distribution in the parasite *Trichomonas vaginalis*. *Cell Microbiol* **2015**, *17*, 1217-1229, doi:10.1111/cmi.12431.
11. Molgora, B.M.; Rai, A.K.; Sweredoski, M.J.; Moradian, A.; Hess, S.; Johnson, P.J. A Novel *Trichomonas vaginalis* Surface Protein Modulates Parasite Attachment via Protein:Host Cell Proteoglycan Interaction. *mBio* **2021**, *12*, doi:10.1128/mBio.03374-20.
12. Thiery, J.P. Mise en evidence des polysaccharides sur coupes fines en microscopie electronique. *J Microsc* **1967**, *6*, 987–1018.
13. Srinivas, M.; Costa, M.; Gao, Y.; Fort, A.; Fishman, G.I.; Spray, DC Voltage dependence of macroscopic and unitary currents of gap junction channels formed by mouse connexin50 expressed in rat neuroblastoma cells. *J Physiol* **1999**, *517*, 673-689, doi:10.1111/j.1469-7793.1999.0673s.x.
14. Chen, Y.P.; Riestra, A.M.; Rai, A.K.; Johnson, P.J. A Novel Cadherin-like Protein Mediates Adherence to and Killing of Host Cells by the Parasite *Trichomonas vaginalis*. *mBio* **2019**, *10*, doi:10.1128/mBio.00720-19.
15. Ryan, C.M.; de Miguel, N.; Johnson, P.J. *Trichomonas vaginalis*: current understanding of host-parasite interactions. *Essays Biochem* **2011**, *51*, 161-175, doi:10.1042/bse0510161.
16. Nievas, YR; Lizarraga, A.; Salas, N.; Cóceres, V.M.; de Miguel, N. Extracellular vesicles released by anaerobic protozoan parasites: Current situation. *Cell Microbiol* **2020**, *22*, e13257, doi:10.1111/cmi.13257.
17. Gold, D.; Ofek, I. Adhesion of *Trichomonas vaginalis* to plastic surfaces: requirement for energy and serum constituents. *Parasitology* **1992**, *105*, 55-62, doi:10.1017/s0031182000073686.
18. Silva Filho, FC; Elias, C.A.; De Souza, W. Role of divalent cations, pH, cytoskeleton components and surface charge on the adhesion of *Trichomonas vaginalis* to a polystyrene substrate. *Mem Inst Oswaldo Cruz* **1987**, *82*, 379-384, doi:10.1590/s0074-02761987000300009.
19. Brugerolle, G.; Bricheux, G.; Coffe, G. Actin cytoskeleton demonstration in *Trichomonas vaginalis* and in other trichomonads. *Biol Cell* **1996**, *88*, 29-36, doi:10.1016/s0248-4900(97)86828-1.
20. Bastida-Corcuera, F.D.; Okumura, C.Y.; Colocoussi, A.; Johnson, P.J. *Trichomonas vaginalis* lipophosphoglycan mutants have reduced adherence and cytotoxicity to human ectocervical cells. *Eukaryot Cell* **2005**, *4*, 1951-1958, doi:10.1128/ec.4.11.1951-1958.2005.
21. Hsu, H.M.; Yang, Y.Y.; Huang, Y.H.; Chu, C.H.; Tu, T.J.; Wu, Y.T.; Chiang, C.J.; Yang, S.B.; Hsu, D.K.; Liu, F.T.; et al. Distinct features of the host-parasite interactions between nonadherent and adherent *Trichomonas vaginalis* isolates. *PLoS Negl Trop Dis* **2023**, *17*, e0011016, doi:10.1371/journal.pntd.0011016.
22. Dos Santos, O.; Rigo, G.V.; Macedo, A.J.; Tasca, T. *Trichomonas vaginalis* clinical isolates: cytoadherence and adherence to polystyrene, intrauterine device, and vaginal ring. *Parasitol Res* **2017**, *116*, 3275-3284, doi:10.1007/s00436-017-5638-0.
23. Salas, N.; Blasco Pedreros, M.; Dos Santos Melo, T.; Maguire, V.G.; Sha, J.; Wohlschlegel, JA; Pereira-Neves, A.; de Miguel, N. Role of cytoneme structures and extracellular vesicles in *Trichomonas vaginalis* parasite-parasite communication. *Elife* **2023**, *12*, doi:10.7554/eLife.86067.
24. Nievas, Y.R.; Vashisht, A.A.; Corvi, M.M.; Metz, S.; Johnson, P.J.; Wohlschlegel, J.A.; de Miguel, N. Protein Palmitoylation Plays an Important Role in *Trichomonas vaginalis* Adherence. *Mol Cell Proteomics* **2018**, *17*, 2229-2241, doi:10.1074/mcp.RA117.000018.

25. Aquino, M.F.K.; Hinderfeld, A.S.; Simoes-Barbosa, A. *Trichomonas vaginalis*. *Trends Parasitol* **2020**, *36*, 646-647, doi:10.1016/j.pt.2020.01.010.
26. Kusdian, G.; Woehle, C.; Martin, W.F.; Gould, S.B. The actin-based machinery of *Trichomonas vaginalis* mediates flagellate-amoeboid transition and migration across host tissue. *Cell Microbiol* **2013**, *15*, 1707-1721, doi:10.1111/cmi.12144.
27. Okumura, C.Y.; Baum, L.G.; Johnson, P.J. Galectin-1 on cervical epithelial cells is a receptor for the sexually transmitted human parasite *Trichomonas vaginalis*. *Cell Microbiol* **2008**, *10*, 2078-2090, doi:10.1111/j.1462-5822.2008.01190.x.
28. Bennett, V.; Baines, A.J. Spectrin and ankyrin-based pathways: metazoan inventions for integrating cells into tissues. *Physiol Rev* **2001**, *81*, 1353-1392, doi:10.1152/physrev.2001.81.3.1353.
29. Cunha, S.R.; Mohler, P.J. Ankyrin protein networks in membrane formation and stabilization. *J Cell Mol Med* **2009**, *13*, 4364-4376, doi:10.1111/j.1582-4934.2009.00943.x.
30. Twu, O.; de Miguel, N.; Lustig, G.; Stevens, G.C.; Vashisht, A.A.; Wohlschlegel, JA; Johnson, P.J. *Trichomonas vaginalis* exosomes deliver cargo to host cells and mediate host∶parasite interactions. *PLoS Pathog* **2013**, *9*, e1003482, doi:10.1371/journal.ppat.1003482.
31. Olmos-Ortiz, L.M.; Barajas-Mendiola, M.A.; Barrios-Rodiles, M.; Castellano, L.E.; Arias-Negrete, S.; Avila, E.E.; Cuéllar-Mata, P. *Trichomonas vaginalis* exosome-like vesicles modify the cytokine profile and reduce inflammation in parasite-infected mice. *Parasite Immunol* **2017**, *39*, doi:10.1111/pim.12426.
32. Rai, A.K.; Johnson, P.J. *Trichomonas vaginalis* extracellular vesicles are internalized by host cells using proteoglycans and caveolin-dependent endocytosis. *Proc Natl Acad Sci USA* **2019**, *116*, 21354-21360, doi:10.1073/pnas.1912356116.
33. Abels, E.R.; Breakefield, X.O. Introduction to Extracellular Vesicles: Biogenesis, RNA Cargo Selection, Content, Release, and Uptake. *Cell Mol Neurobiol* **2016**, *36*, 301-312, doi:10.1007/s10571-016-0366-z.